

Wavepacket dynamics in energy space, RMT and Quantum-Classical correspondence

Doron Cohen¹, Felix M. Izrailev² and Tsampikos Kottos³

¹ Department of Physics, Harvard University, Cambridge, MA 02138

² Instituto de Fisica, Universidad Autonoma de Puebla, Puebla, Pue 72570, Mexico

³ Max-Planck-Institut für Strömungsforschung, 37073 Göttingen, Germany

(September 1999)

We apply random-matrix-theory (RMT) to the analysis of evolution of wavepackets in energy space. We study the crossover from ballistic behavior to saturation, the possibility of having an intermediate diffusive behavior, and the feasibility of strong localization effect. Both theoretical considerations and numerical results are presented. Using quantal-classical correspondence (QCC) considerations we question the validity of the emerging dynamical picture. In particular we claim that the appearance of the intermediate diffusive behavior is possibly an artifact of the RMT strategy.

We are interested in the dynamics that is generated by a Hamiltonian of the type $\mathcal{H} = \mathbf{E} + \mathbf{W}$ where \mathbf{E} is a diagonal matrix whose elements are the ordered energies $\{E_n\}$, with mean level spacing Δ , and \mathbf{W} is a banded matrix. It is assumed that \mathbf{W} is similar to a ‘Banded Random Matrix’ (BRM), with non-vanishing couplings within the band $0 < |n - m| \leq b$. These coupling elements are zero on the average, and they are characterized by the variance $v = \langle (|\mathbf{W}_{nm}|^2) \rangle^{1/2}$. Thus, there are three parameters (Δ, b, v) that controls the dynamics.

One important application of BRM is in solid-state physics for the study of localization in quasi-one-dimensional disordered systems. In this frame non-zero values of Δ reflect the presence of a constant electric field along the sample. However, in this Letter we mainly have in mind the original motivation that has been introduced by Wigner [1] forty years ago: Namely, the study of complex conservative quantum systems that are encountered in nuclear physics as well as in atomic and molecular physics. For this reason the above defined model (with non-zero Δ) is known in the literature [2–4] as Wigner’s BRM (WBRM) model.

Below we define the classical system, as well as the classical scenario, and specify the \hbar dependence of the associated WBRM-model parameters. Then we define the various parametric regimes in the quantum-mechanical theory, and we analyze the corresponding dynamical scenarios. In the last paragraph we explain that the emerging picture is incompatible with the quantal-classical correspondence (QCC) principle. Both the terminology and the notations that are used in this Letter are intended to make our final observation as transparent as possible.

In actual physical applications that we have in mind, \mathcal{H} is determined via a ‘quantization’ of a classical Hamiltonian. At $t = 0$ the system is prepared in an eigenstate of a Hamiltonian \mathcal{H}_0 . For $t > 0$ the evolution of the system is determined by the total Hamiltonian \mathcal{H} . The evolving state is $\psi(t)$, and we are interested in the study of the evolving distribution $|\langle n|\psi(t)\rangle|^2$. We assume that both \mathcal{H}_0 and \mathcal{H} generate in the classical limit chaotic dynamics of similar nature. According to semiclassical arguments [2], the Hamiltonian matrix \mathcal{H} in the basis that is determined by \mathcal{H}_0 has a band structure which may be approximated by that of a WBRM. The \hbar dependence of the three parameters that define the effective WBRM

model is easily determined [2]. One obtains $\Delta \propto \hbar^d$, and $b \propto \hbar^{-(d-1)}$, and $v \propto \hbar^{(d-1)/2}$, where d is the number of degrees of freedom (dimensionality) of the system. In the corresponding classical model there are two significant parameters:

$$\tau_{\text{cl}} = \hbar/(b\Delta) , \quad \delta E_{\text{cl}} = 2\sqrt{bv} \quad (1)$$

Both parameters have a very simple interpretation: Once we use \mathcal{H} as a generator for the (classical) dynamics, the energy $\mathcal{H}_0(t)$ fluctuates. The fluctuations are characterized by the correlation time τ_{cl} , and by the amplitude δE_{cl} . The classical scenario is easily figured out by using a phase-space picture [5]: The initial preparation corresponds to a microcanonical distribution that is supported by one of the energy-surfaces of the \mathcal{H}_0 Hamiltonian. For $t > 0$, the phase-space distribution spreads away from the initial surface. ‘Points’ of the evolving distribution move upon the energy-surfaces of the \mathcal{H} Hamiltonian. Then, due to ergodicity, a ‘steady-state distribution’ appears, where the evolving ‘points’ occupies an ‘energy shell’ in phase-space. We are interested in the distribution of the energies $\mathcal{H}_0(t)$ of the evolving ‘points’. One expects that for short times this energy distribution evolves in a ballistic fashion, and later, once ergodic ‘steady-state’ appears, there is a saturation. The saturation time and the saturation scale are τ_{cl} and δE_{cl} respectively.

Below we are going to study the corresponding quantum-mechanical scenario. We shall use the following terminology: The standard perturbative regime is $(v/\Delta) \ll 1$; The Wigner regime is $1 \ll (v/\Delta) \ll b^{1/2}$; The ergodic regime is $b^{1/2} \ll (v/\Delta) \ll b^{3/2}$; The localization regime is $b^{3/2} \ll (v/\Delta)$. It is easily verified that the limit $\hbar \rightarrow 0$ corresponds to the ergodic regime or possibly (provided $d = 2$) to the localization regime.

The structure of the eigenstates α of \mathcal{H} has been studied in [1,3,4]. We denote the average shape of an eigenstate as $W_E(r) = \langle |\varphi_\alpha(n_\alpha + r)|^2 \rangle$ where $\varphi_\alpha(n) = \langle n|\alpha\rangle$, and n_α is the ‘site’ around which the eigenstate is located. The average is taken over all the eigenstates that have roughly the same energy $E_\alpha \sim E$. There are two important energy scales: One is the classical width of the energy shell δE_{cl} , and the other is the range of the interaction $\Delta_b = b\Delta$. In the *standard perturbative regime* $W_E(r)$ contains mainly one level, and there are perturbative tails that extend over the range Δ_b . In the *Wigner regime*,

many levels are mixed: the main (non-perturbative) component of $W_E(r)$ has width $\Gamma = 2\pi(v/\Delta)^2 \times \Delta$, and the shape within the bandwidth Δ_b is of Lorentzian type. However in actual physical applications this Lorentzian is a special case of core-tail structure [5,6], where the tail can be found via first order perturbation theory. Outside the bandwidth the tails decay faster than exponentially [3]. On approach to the ergodic regime $W_E(r)$ spills over the range Δ_b . Deep in the *ergodic regime* it occupies ‘ergodically’ the whole energy shell whose width is δE_{cl} . In actual physical applications the exact shape is determined by simple classical considerations [5–7]. Deep in the *localization regime* $W_E(r)$ is no longer ergodic: A typical eigenstate is exponentially localized within an energy range $\delta E_\xi = \xi\Delta$ much smaller than δE_{cl} . The localization length is $\xi \approx b^2$. In actual physical applications it is not clear whether there is such type of localization. To avoid confusion, we are going to use the term ‘localization’ only in the sense of having $\delta E_\xi \ll \delta E_{cl}$.

Now we would like to explore the various dynamical scenarios that can be generated by the Schrödinger equation for $a_n(t) = \langle n|\psi(t)\rangle$. Namely,

$$\frac{da_n}{dt} = -\frac{i}{\hbar} E_n a_n - \frac{i}{\hbar} \sum_m \mathbf{W}_{nm} a_m \quad (2)$$

starting with an initial preparation $a_n = \delta_{nm}$ at $t=0$. Without loss of generality we fix the variance ($v=1$). In a previous study [8] only the localization regime ($\Delta = 0$) has been considered. Here we are going to consider the general case ($\Delta \neq 0$). We describe the energy spreading profile for $t > 0$ by the transition probability kernel $P_t(n|m) = \langle |a_n(t)|^2 \rangle$. The angular brackets stand for averaging over realizations of the Hamiltonian. In particular, it is convenient to characterize the energy spreading profile by the second moment $M(t) = \sum_n (n-m)^2 P_t(n|m)$, and by the participation ratio $N(t) = (\sum_n (P_t(n|m))^2)^{-1}$, and by the total transition probability $p(t)$, and by the out-of-band transition probability $q(t)$. Both $p(t)$ and $q(t)$ are defined as $\sum'_n P(n|m)$ where the prime indicate exclusions of the term $n = m$ or exclusion of the terms $|n-m| > b$ respectively. Equation (2) has been integrated numerically using the self-expanding algorithm of reference [8] to eliminate finite-size effects. Fig.1 illustrates the time-evolution of the energy spreading profile. From such plots we can define various time scales. The times t_{ball} and t_{sat} pertains to $M(t)$ and mark the departure-time from ballistic behavior and the crossover-time to saturation. The time t_{sta} pertains to $N(t)$ and marks the crossover to a stationary distribution. The time scale t_{prt} pertains to $p(t)$ and marks the disappearance of the simple perturbative structure (See (3) below). The asymptotic value of $q(t)$, if it is much less than 1, indicates that the system is either in the standard perturbative regime or in the Wigner regime, where out-of-band transitions can be neglected. The saturation profile is given by the expression $P_\infty(n|m) = \sum_\alpha |\langle n|\alpha \rangle|^2 |\langle \alpha|m \rangle|^2$, and it is roughly approximated by the auto-convolution of $W_E(r)$. There-

fore the saturation profile is expected to be similar to the average shape of the eigenstates. Fig.2 displays representative saturation profiles. We have found out (Fig.2e) that $M(\infty)$ satisfies a scaling relation similar to the one that pertains to the average shape of the eigenstates [4].

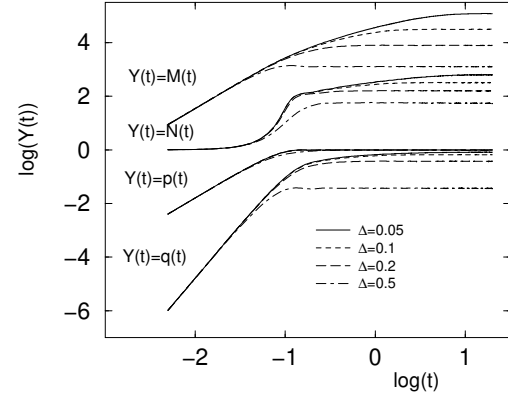


FIG. 1. Representative examples for the time-evolution of the energy spreading profile. The second moment $M(t)$, the participation ratio $N(t)$, the total transition probability $p(t)$, and the out-of-band transition probability $q(t)$ are plotted for $\Delta = 0.05, 0.10, 0.20, 0.50$ while $v = 1$ and $b = 80$.

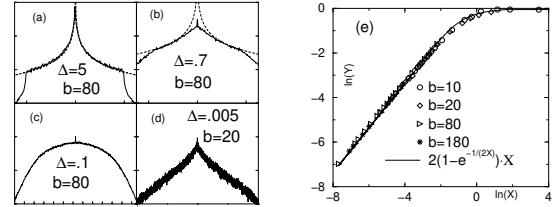


FIG. 2. *Left figures:* Saturation profiles for various regimes: (a) Standard perturbative regime; (b) Wigner regime; (c) Ergodic regime; (d) Localization regime. The distance between the tick-marks on the horizontal axis of (a)-(c) is b . In (d) the full scale is $|n-m| < 2000$. The full scale of the vertical log-axis is $-15 < \ln(P) < 0$. Note that the $n=m$ term is factor 3 larger compared with its immediate vicinity [8]. In (a) and (b) the $1/(n-m)^2$ behavior of the (in-band) tail is fitted by dashed lines. Notice the appearance of a core region in (b), indicated by the ‘flattening’ of the profile for $|n-m| < 20$. The in-band profile corresponds to a Lorentzian with a very high accuracy. The *right figure* (e) displays $Y = (M(\infty))^{1/2}/b^2$ versus $X = (v/\Delta)/b^{3/2}$. The solid-line illustrates the scaling relation, similar to that of [4].

Let us start with the *standard perturbative regime* where each eigenstate of \mathcal{H} is localized ‘perturbatively’ in one energy level. Thus, for arbitrarily long times the probability is concentrated mainly in the initial level. We can write schematically

$$P_t(n|m) \approx \delta_{nm} + \text{Tail}(n-m; t) \quad (3)$$

where $\text{Tail}(n-m; t)$ is non-zero only for first order transitions ($0 < |n-m| < b$), and its total normalization is much less than unity. The explicit expression for the tail probabilities is [5]:

$$\text{Tail}(n-m; t) = \left(\frac{v}{\hbar}\right)^2 t \tilde{F}_t \left(\frac{E_n - E_m}{\hbar}\right) \quad (4)$$

where $\tilde{F}_t(\omega) = t \cdot (\text{sinc}(\omega t/2))^2$ is the spectral-content of a constant perturbation whose duration is t . We have trivial type of recurrences from n to m once t becomes larger compared with $2\pi\hbar/(E_n - E_m)$. The global crossover to quasi-periodic behavior is marked by the Heisenberg time $t_H = 2\pi\hbar/\Delta$ (see Fig.3).

In the *Wigner regime*, one observes that the perturbative expression (3) is still valid for sufficiently short times $t \ll t_{\text{prt}}$. Let us estimate the perturbative break-time t_{prt} . For short times ($t < \tau_{\text{cl}}$) the spectral function $\tilde{F}_t(\omega)$ is very wide compared with the bandwidth Δ_b of first-order transitions. Consequently we can use the replacement $\tilde{F}_t(\omega) \mapsto t$ and we get that the total transition probability is $p(t) \approx b \times (vt/\hbar)^2$. On the other hand, for $t > \tau_{\text{cl}}$, the spectral function $\tilde{F}_t(\omega)$ is narrow compared with the bandwidth, and it can be approximated by a delta-function. As a result we get $p(t) \approx v^2/(\hbar\Delta) \times t$. We can determine t_{prt} via the condition $p(t) \sim 1$. The result is

$$t_{\text{prt}} = \begin{cases} \hbar\Delta/v^2 & \text{for } 1 < v/\Delta < \sqrt{b} \\ \hbar/(\sqrt{b}v) & \text{for } \sqrt{b} < v/\Delta \end{cases} \quad (5)$$

It should be noticed that for $v \sim \Delta$ we get $t_{\text{prt}} \sim t_H$. Thus, taking recurrences into account, we come again to the conclusion, that for $v \ll \Delta$ there is no perturbative breaktime. The *second moment* $(\delta E(t))^2 = \Delta^2 \times M(t)$ of the energy distribution (3) is easily calculated. We get a ballistic-like behavior, followed by saturation,

$$\delta E(t) \approx \begin{cases} (\delta E_{\text{cl}}/\tau_{\text{cl}}) t & \text{for } t < \tau_{\text{cl}} \\ \delta E_{\text{cl}} & \text{for } t > \tau_{\text{cl}} \end{cases} \quad (6)$$

For $t \sim t_{\text{prt}}$ the tail (4) becomes Lorentzian-like, and it is characterized by a width $\hbar/t = \Gamma$. For $t > t_{\text{prt}}$ expression (3) losses its validity, but it is obvious that the energy cannot spread any more, since it had already acquired the saturation profile.

It should be realized that neither (3), nor the Lorentzian-like saturation profile, could correspond to the classical spreading profile. In particular, note that the saturation profile in the Wigner regime is characterized by two genuine quantum mechanical scales (Γ, Δ_b), whereas the classical ergodic distribution is characterized by the single energy scale δE_{cl} . However, in spite of this lack of correspondence, the second moment (6) behaves in a classical-like fashion. Using the terminology of [5] we have here *restricted* rather than *detailed* quantal-classical correspondence (QCC): The quantal $P_t(n|m)$ is definitely different from its classical analog, but the *second moment* turns out to be the same.

In the *ergodic regime* the time scale τ_{cl} becomes larger than t_{prt} , and therefore τ_{cl} loses its significance. At $t \sim t_{\text{prt}}$ the quantal energy-spreading just "fills" the energy range Δ_b , and we get $\delta E(t) \approx \Delta_b$. The perturbative result (3) is no longer applicable for $t > t_{\text{prt}}$. However, the simplest heuristic picture turns out to be correct.

Namely, once the mechanism for ballistic-like spreading disappears a stochastic-like behavior takes its place. The stochastic energy spreading is similar to a random-walk process where the step size is of the order b , with transient time equals t_{prt} . Therefore we have a diffusive behavior $M(t) = D_n t$ where

$$D_n = C \cdot b^2/t_{\text{prt}} = C \cdot b^{5/2}v/\hbar \quad (7)$$

and the numerical prefactor [8] is $C \approx 0.85$. It should be observed that the diffusion is not of classical nature since $D_E = \Delta^2 \times D_n \propto \hbar$. This diffusion can go on as long as $(D_E t)^{1/2} < \delta E_{\text{cl}}$. This defines an ergodic time

$$t_{\text{erg}} = b^{-3/2} \hbar v/\Delta^2 \propto 1/\hbar \quad (8)$$

After the ergodic time the energy spreading profile saturates to a classical-like steady state distribution [4].

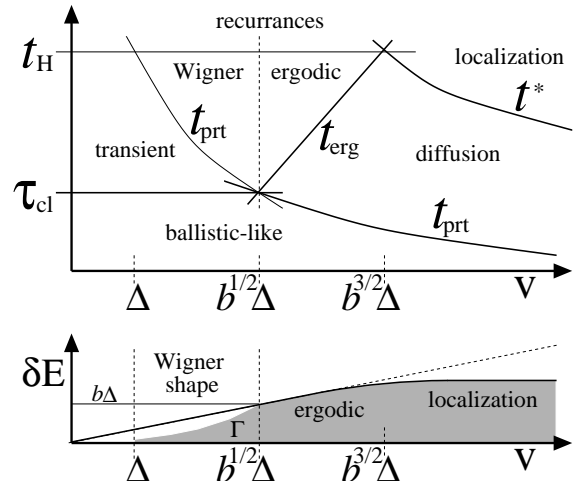


FIG. 3. The *upper diagram* illustrates the various dynamical scenarios which are described in the text. The flow of time is in the vertical direction. See [9] for closely related diagrams. The *lower plot* illustrates the various energy-scales that characterize the associated stationary distributions: The bandwidth Δ_b is indicated by a horizontal solid line; The width of the non-perturbative component is indicated by the grey filling; The width of the energy shell is indicated by the dashed line; The second moment $\delta E(\infty)$ is indicated by the bold solid line. In the localization regime we have $\delta E(\infty) \approx \delta E_\xi \ll \delta E_{\text{cl}}$. The numerical data for $\delta E(\infty)$ are presented in both Fig.2e and Fig4b.

In the *localization regime* the quasi periodic nature of the dynamics is important. The 'operative' eigenstates are defined as those having a non-negligible overlap with the initial state m . These eigenstates are located within the energy shell whose width is δE_{cl} . If the eigenstates within the energy shell are ergodic, then all of them are 'operative', and therefore the effective level spacing between them is simply $\Delta_{\text{eff}} \approx \Delta$. However, if the eigenstates within the energy shell are localized, then only ξ out of them have a significant overlap with the initial state m , and therefore the effective level spacing is $\Delta_{\text{eff}} \approx \delta E_{\text{cl}}/\xi$. The effective energy spacing Δ_{eff} is the relevant energy scale for determination of the crossover

to quasiperiodic behavior. The associated time scale is $t^* = 2\pi\hbar/\Delta_{\text{eff}}$, and it may be either less than or equal to the Heisenberg time $t_H = 2\pi\hbar/\Delta$. The localization regime is defined by the condition $t^* < t_{\text{erg}}$. In this regime the diffusion stops before an ergodic distribution arises, and we should get $D_n t^* \approx \xi^2$. Inserting the definition of t^* and solving for ξ we obtain the well known [2,4] estimate $\xi \approx b^2$. For the breaktime we obtain

$$t^* = b^{3/2}\hbar/v \propto (1/\hbar)^{2d-3} \quad (9)$$

Note that the localization range is $\delta E_\xi = \xi\Delta \propto (1/\hbar)^{d-2}$. If the diffusion were of classical nature, we would get $\delta E_\xi \propto (1/\hbar)^{d-1}$ as in the semiclassical analysis of [9].

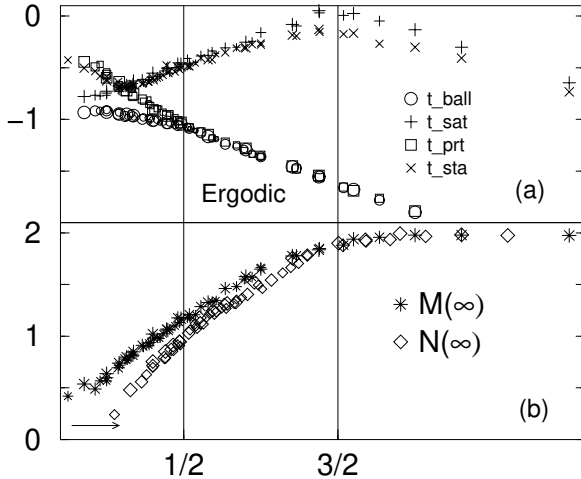


FIG. 4. (a) The times t_{ball} , t_{sat} , t_{sta} and t_{prt} are numerically determined. Different values of b are distinguished by the relative size of the symbols. The horizontal axis is $X = \log(v/\Delta)/\log(b)$, and the vertical axis is $Y = \log(t/t_H)/\log(2\pi)$. (Note that $Y = -1$ implies $t = \tau_{\text{cl}}$). In the Wigner regime both t_{ball} and t_{sat} are of the order τ_{cl} , up to a constant factor. At the same regime t_{sta} coincides with t_{prt} . As we move toward the ergodic regime t_{sat} departs from t_{ball} and joins t_{sta} . As a consequence an intermediate diffusive regime appears, involving a premature departure of the ballistic behavior at $t_{\text{ball}} \sim t_{\text{prt}}$. Increasing X further, t_{sat} and t_{sta} approach t_H but eventually drop down to lower values. This is due to the crossover from the ergodic to the localization regime as implied by Fig.3a. (b) Both $\log(M(\infty))/\log(b)$ and $\log(N(\infty))/\log(b)$ are plotted versus $\log(v/\Delta)/\log(b)$. This corresponds to Fig.3b. The arrow indicates a global horizontal shift of the $N(\infty)$ plot for presentation purpose.

The various dynamical scenarios discussed above are summarized by the diagram of Fig.3, and can be compared with the data presented in Fig.4. We come back now to the ‘physics’ and recall that WBRM should model the actual dynamics that is generated by some ‘quantized’ Hamiltonian. The condition to be in the regime $(v/\Delta) \ll b^{1/2}$ can be cast into the form $\hbar \gg C_{\text{prt}}$, where C_{prt} is a classical scale. In this regime we have restricted QCC and (6) holds. This equation is valid also in case of the ‘quantized’ Hamiltonian, since its derivation is

not sensitive to the presence or the absence of subtle correlations between matrix elements. In contrast to that, in the *non-perturbative* regime $\hbar \ll C_{\text{prt}}$, these correlations become important, and it may have implications on the dynamical behavior.

Fixing all the classical parameters, including the time t which is assumed to be of the order of τ_{cl} , we can always define a sufficient condition for having detailed QCC, and cast this condition into the form $\hbar \ll C_{\text{sc}}$, where C_{sc} is another classical scale. (See [5] for a closely related discussion). The parameter C_{sc} is, in general, non-universal (system-specific) parameter. Thus for $\hbar \ll C_{\text{sc}}$ we have detailed QCC and therefore (6) should hold again.

The WBRM model which has been discussed in this Letter predicts that for $\hbar \ll C_{\text{prt}}$ there is a pre-mature departure from ballistic behavior, and an intermediate diffusive behavior. So we have a contradiction here between RMT considerations on one hand, and QCC semiclassical considerations on the other. Thus, if the RMT approach is non-trivially valid, then it is only in a restricted range $C_{\text{sc}} \ll \hbar \ll C_{\text{prt}}$. Outside this regime it is either trivially valid ($\hbar \gg C_{\text{prt}}$) and we have restricted QCC, or else it is not valid at all ($\hbar \ll C_{\text{sc}}$) and we have detailed QCC.

It may be true that in many cases the RMT considerations are not valid for the purpose of analyzing time-dependent dynamical scenarios. A similar situation may arise in the theory of quantum dissipation: There is one-to-one correspondence between the regimes in Fig.5 of [5] and the regimes that have been discussed in this Letter.

We thank the MPI für Komplexe Systeme in Dresden for the kind hospitality during the Conference *Dynamics of Complex Systems* where this work was initiated. F.M.I acknowledges support by CONACyT (Mexico) Grants No. 26163-E and 28626-E.

- [1] E. Wigner, Ann. Math **62** 548 (1955); **65** 203 (1957).
- [2] M. Feingold and A. Peres, Phys. Rev. A **34** 591, (1986). M. Feingold, D. Leitner, M. Wilkinson, Phys. Rev. Lett. **66**, 986 (1991); M. Wilkinson, M. Feingold, D. Leitner, J. Phys. A **24**, 175 (1991); M. Feingold, A. Gioletta, F. M. Izrailev, L. Molinari, Phys. Rev. Lett. **70**, 2936 (1993).
- [3] V.V. Flambaum, A.A. Gribakina, G.F. Gribakin and M.G. Kozlov, Phys. Rev. A **50** 267 (1994).
- [4] G. Casati, B.V. Chirikov, I. Guarneri and F.M. Izrailev, Phys. Rev. E **48**, R1613 (1993); Phys. Lett. A **223**, 430 (1996).
- [5] D. Cohen, Phys. Rev. Lett. **82**, 4951 (1999); cond-mat/9902168.
- [6] D. Cohen and E. Heller, preprint (1999).
- [7] F. Borgonovi, I. Guarneri and F.M. Izrailev Phys. Rev. E **57**, 5291 (1998).
- [8] F. M. Izrailev, T. Kottos, A. Politi, S. Ruffo and G. P. Tsironis, Europhys. Lett. **34**, 441 (1996). F.M. Izrailev, T. Kottos, A. Politi and G.P. Tsironis, Phys. Rev. E **55**, 4951 (1997).
- [9] D. Cohen, J. Phys. A **31**, 277 (1998).